Textile & Leather Review

ISSN 2623-6281 | www.tlr-journal.com | 10.31881/TLR

UAV Flight and Deployment Strategies Based on a Cooperative-Guidance and Global-Perturbation Particle Swarm Optimization Algorithm

Mengshi Ma, Hongjun Tian, Tao Zhu, Guijie Liu

How to cite: MA M, Tian H, Zhu T, Liu G. UAV Flight and Deployment Strategies Based on a Cooperative-Guidance and Global-Perturbation Particle Swarm Optimization Algorithm. Textile & Leather Review. 2026; 9:2235-2259. https://doi.org/10.31881/TLR.2026.2235

How to link: https://doi.org/10.31881/TLR.2026.2235

Published: 25 April 2026

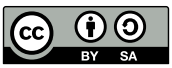

UAV Flight and Deployment Strategies Based on a Cooperative-Guidance and Global-Perturbation Particle Swarm Optimization Algorithm

Mengshi Ma[1], Hongjun Tian[1]*, Tao Zhu[1], Guijie Liu[2]

[1]College of Engineering Science and Technology, Shanghai Ocean University, Shanghai 201306, China.

[2]College of Engineering, Ocean University of China, Qingdao 266100, China.

*tianhongjun86@163.com

Article

https://doi.org/10.31881/TLR.2026.2235

Published 25 April 2026

ABSTRACT

In multi-missile attack scenarios, UAV swarms face a challenging cooperative decision-making problem when deploying smoke munitions to interfere with missile guidance systems. Focusing on the maximization of effective visual obscuration duration, this paper investigates the coordinated planning of UAV flight trajectories and smoke munition deployment strategies. First, the three-dimensional motion and interaction processes of UAVs, missiles, and smoke munitions are modeled in the time domain, and a high-dimensional nonlinear cooperative optimization model is established. Then, to address the dimensional explosion and local optimum issues encountered in model solving, as well as the difficulty of handling simulation-based, non-analytical objective functions, an improved particle swarm optimization algorithm integrating a cooperative-guidance mechanism and a global-perturbation strategy is developed. Combined with threat-level assessment and a greedy resource allocation strategy, a hierarchical solution framework is proposed. Simulation results demonstrate the effectiveness of the proposed method, showing that it can efficiently generate optimal resource allocation schemes and cooperative UAV interference strategies, achieve superior interference performance in complex adversarial scenarios, and exhibit good engineering applicability and potential for practical deployment.

KEYWORDS

UAV cooperation, particle swarm optimization, cooperative guidance, high-dimensional nonlinear optimization

INTRODUCTION

With the rapid advancement of science and technology, precision-guided weapons and unmanned combat platforms have been increasingly deployed in modern warfare. Effectively mitigating the threat posed by incoming missiles under complex operational environments has thus become a critical issue that modern

defense systems urgently need to address. As a representative soft-kill countermeasure, smoke munitions can rapidly form obscuration regions to interfere with missile guidance processes [1]. When deployed via UAV platforms, they have gradually become an essential component of air defense systems due to advantages such as high maneuverability and controllable operational costs [2]. However, under complex scenarios involving multiple missiles arriving simultaneously and constrained operational time windows, how to rationally coordinate multiple UAVs to cooperatively deploy smoke munitions so as to maximize the effective interference duration remains a highly challenging engineering optimization problem [3–5].

Existing studies have mainly focused on the application mechanisms of smoke-munition interference in missile defense, covering key issues such as obscuration-condition identification and factor analysis of interference duration, and have also explored optimization strategies for deployment trajectories and parameters under specific constraints [6–8]. Some works model UAV-based smoke-munition deployment as an optimization problem with spatial and/or temporal constraints, and validate the interference effectiveness in scenarios involving a single platform and limited munitions via simulations [9–11]. With further research progress, cooperative combat scenarios with multiple UAVs and multiple munitions have gradually attracted increasing attention, where coordinated effectiveness is often assessed by aggregating or superimposing the interference intervals of smoke munitions [12–13]. However, as the dimensionality of decision variables increases in cooperative settings, the difficulty of solving the model grows exponentially. Existing approaches typically either integrate UAV flight and deployment decisions within a unified planning model, or adopt distributed modeling to plan the decisions of each UAV separately to achieve global coordination; such methods generally rely on heuristic or metaheuristic algorithms for solving [14–19]. Nevertheless, in practical applications, the evaluation of smoke-obscuration effectiveness depends on time-domain simulation, which makes the objective function difficult to express in an analytical form and thus limits the applicability of conventional intelligent optimization algorithms. As a result, existing methods may face challenges in maintaining global search performance and computational scalability when applied to such simulation-driven problems.

To address the above research gaps, this paper focuses on the joint spatiotemporal parameter optimization problem in UAV-based smoke-munition deployment interference. By constructing a three-dimensional time-domain simulation model, the coupled motion relationships among UAVs, missiles, and smoke clouds are accurately characterized. Taking effective obscuration duration as the core performance metric, an optimization model is established with continuous decision variables and temporal constraints. Based on this model,

systematic simulation-based solution studies are conducted for different operational scenarios, including single-platform–single-munition and multi-platform–multi-munition settings. To overcome the global optimization difficulty caused by the increased model dimensionality, a cooperative-guidance mechanism and a global-perturbation strategy are incorporated into the particle swarm optimization framework. In combination with a threat assessment model and resource allocation considerations, a hierarchical solution strategy suitable for complex scenarios is proposed.

THEORETICAL FRAMEWORK AND METHODOLOGY

This paper considers the interference of incoming missiles through UAV-deployed smoke munitions in a three-dimensional space. Visual obscuration is generated to delay the missile guidance process toward the real target. The objective is to maximize the effective obscuration duration, thereby increasing the likelihood that the missile is guided toward a decoy target. The operational space is defined as the three-dimensional Euclidean space $\mathbb{R}^3$, and the time variable t is treated as a continuous variable; multiple UAVs carrying smoke munitions with delayed detonation capability release smoke at appropriate times and spatial locations, thereby forming visual obscuration along the line of sight between the missile and the real target. Let the set of missiles be denoted as $\mathcal{M} = \{1, ..., M\}$, and let the mission time horizon be $t \in [0, T]$. An obscuration indicator function $I(t)$ is introduced, where $I(t) = 1$ if the missile line of sight is blocked by smoke at time t , and $I(t) = 0$ otherwise. Accordingly, the total effective obscuration duration T_e is defined as the integral of this indicator function over the effective lifetime of the smoke cloud:

$$T_e = \int_{t_{det}}^{t_{end}} I(t)dt \approx \sum_{k=0}^{N-1} I(t_k) \cdot \Delta t \tag{1}$$

Here, $t_k = t_{\text{det}} + k \cdot \Delta t$, and all-time steps are traversed within the simulation loop to obtain the effective obscuration duration. For the case where multiple smoke munitions interfere with a single missile, the effective obscuration interval of the k -th smoke munition under the decision vector $\vec{X}$ is denoted as $I_k(\vec{X})$. Accordingly, the mathematical expression of the objective function, namely the total effective obscuration duration $f(\vec{X})$, is given as:

$$\max f(\vec{X}) = \text{length}\left(\bigcup_{k=1}^{n} I_k(\vec{X})\right) \tag{2}$$

This function automatically handles overlapping intervals and computes the true total obscuration duration. In evaluating this function, $I_k(\vec{X})$ denotes the cooperative obscuration indicator function, indicating that at least one smoke munition indexed by k is effective at time t .

Based on the above definitions, this paper focuses on the problem of maximizing the effective joint obscuration duration by appropriately scheduling UAV flight trajectories and smoke-munition deployment strategies under specific operational scenarios and physical constraints. To this end, physical motion models of the involved elements are first established. In a three-dimensional Euclidean space $\mathbb{R}^3$ with the decoy target taken as the origin, missile M_i departs from the initial position $\vec{P}_{M_i,0}$ and moves toward the decoy target along a straight line with a constant speed v_M ; its velocity vector can thus be expressed as:

$$\overrightarrow{v_{Mi}} = v_M \cdot \frac{\overrightarrow{P_{t,fa}} - \overrightarrow{P_{Mi,0}}}{|\overrightarrow{P_{t,fa}} - \overrightarrow{P_{Mi,0}}|} = v_M \cdot \frac{-\overrightarrow{P_{Mi,0}}}{|\overrightarrow{P_{Mi,0}}|} \tag{3}$$

At time t , its position can be expressed as:

$$\overrightarrow{P_{Mi}}(t) = \overrightarrow{P_{Mi,0}} + \overrightarrow{v_M} \cdot t \tag{4}$$

UAV f_i departs from the initial position $\vec{P}_{f_i,0}$ and performs constant-speed straight-line flight at a fixed altitude with speed v_{f_i} , following the same modeling logic as that of the missile motion. Its velocity vector $\vec{v}_{f_i}$ is given by:

$$\overrightarrow{v_{fi}} = v_{f_i} \cdot \frac{\overrightarrow{P_{fi,t}} - \overrightarrow{P_{fi,0}}}{|\overrightarrow{P_{fi,t}} - \overrightarrow{P_{fi,0}}|} \tag{5}$$

The position of UAV f_i at time t can be expressed as $\vec{P}_{f_i}(t)$:

$$\overrightarrow{P_{fi}}(t) = \overrightarrow{P_{fi,0}} + \overrightarrow{v_{fi}} \cdot t \tag{6}$$

After the mission starts, the UAV deploys a smoke munition at time t_d , and the deployment point coordinate $\vec{P}_d$ is given by the UAV position at that time:

$$\vec{P}_d = \overrightarrow{P_{fi}}(t_d) \tag{7}$$

After separating from the UAV, the smoke munition has an initial velocity equal to $\vec{v}_{f_i}$. Subsequently, under the action of gravity, the smoke munition undergoes projectile motion. After a time interval of Δt following deployment, its spatial position $\vec{P}_g(\Delta t)$ is given by:

$$\vec{P}_g(\Delta t) = \vec{P}_d + \overrightarrow{v_{fi}} \cdot \Delta t + \frac{1}{2}\vec{g} \cdot (\Delta t)^2 \tag{8}$$

The smoke munition detonates after a delay of Δd ; therefore, the detonation time t_{det} is given by:

$$t_{det} = t_d + \Delta d \tag{9}$$

Substituting $\Delta t = \Delta d$ into the smoke-munition trajectory equation yields the detonation-point coordinate $\vec{P}_{\mathrm{det}}$:

$$\overrightarrow{P_{det}} = \vec{P}_d + \overrightarrow{v_{fi}} \cdot \Delta d + \frac{1}{2}\vec{g} \cdot (\Delta d)^2 \tag{10}$$

After detonation, the smoke forms a spherical cloud with radius R and descends vertically at a speed v_s . The vertical descent of the smoke cloud with a constant speed is adopted as a simplified assumption to facilitate model tractability. In practical scenarios, environmental factors such as wind and atmospheric turbulence may influence smoke dispersion, which may affect the actual effectiveness of the optimized deployment strategy. This limitation has been explicitly discussed in the Conclusions and Future Work section and will be addressed in future research. At any time t , the center of the smoke cloud $\vec{P}_c(t)$ is given by:

$$\vec{P}_c(t) = \overrightarrow{P_{det}} + (0, 0, -v_s) \cdot (t - t_{det}) \tag{11}$$

Where the time variable t lies in the interval $[t_{det}, t_{end}]$.

It should be noted that the constant-velocity linear motion model adopted in this study serves as a first-order approximation for tractability. In practical scenarios, more complex maneuvering dynamics (e.g., proportional navigation for missiles and aerodynamic disturbances for UAVs) may influence the system behavior.

In model formulation and solution, determining whether effective obscuration is achieved is a key step, as it directly affects the objective-function value of optimization. Effective obscuration requires that, at a given time instant, all lines of sight from the missile to the target cylinder are blocked by the smoke cloud. Here, an approximate method—namely, the discretized sampling approach—is introduced by discretizing the target cylinder into a set of representative sampling points S_T . Specifically, four extreme points on the top base and four extreme points on the bottom base of the cylinder that are parallel to the coordinate axes are selected, yielding a total of eight points. The coordinate set is given as:

$$S_T = \{(0 \pm R_t, Y_t, 0), (0, Y_t \pm R_t, 0), (0 \pm R_t, Y_t, H_t), (0, Y_t \pm R_t, H_t)\} \tag{12}$$

To determine whether complete effective obscuration is achieved at any time instant within the effective lifetime of the smoke, the following condition must be satisfied: for each sampling point $\vec{P}_{T,i} \in S_T$, the line of sight connecting the missile position $\vec{P}_{M_i}(t)$ and the sampling point—i.e., the viewing-direction vector $\overrightarrow{\overrightarrow{P_{Mi}}(t)\overrightarrow{P_{T,i}}}$ —should intersect the smoke-cloud sphere centered at $\vec{P}_c(t)$ with radius R_s . In geometric terms, this is equivalent to requiring that the shortest distance from the smoke-cloud center to each line of sight is less than the smoke radius:

$$\forall \overrightarrow{P_{T,i}} \in S_T, d_{min}(\vec{P}_c(t), \overrightarrow{\overrightarrow{P_{Mi}}(t)\overrightarrow{P_{T,i}}}) \leq R_s \tag{13}$$

Based on the above criterion, an indicator function is introduced as follows:

$$I_{coop}(t, \vec{X}) = \{1, \ \ There\ exists\ at\ least\ one\ k for\ which\ it\ is\ effective\ at\ time\ t \\ 0, \ \ otherwise \tag{14}$$

This indicator function is used to characterize the instantaneous interference state of the smoke on the missile guidance process and provides the basis for the subsequent calculation of the effective obscuration duration. Based on the aforementioned motion models and obscuration determination criteria, the decision-planning problem of UAV smoke-munition deployment is formulated as a high-dimensional nonlinear optimization problem with the objective of maximizing the joint effective obscuration duration. For an operational mission

in which a formation consisting of i UAVs cooperatively deploys k smoke munitions, the complete strategy can be represented by a D -dimensional decision vector $\vec{X}$:

$$\vec{X} = (v_{f1}, \theta_1, ..., v_{fi}, \theta_i, t_d^{(1)}, \Delta d^{(1)}, ..., t_d^{(k)}, \Delta d^{(k)}) \tag{15}$$

Here, $v_{f_i} \in [v_{min}, v_{max}]$ denotes the flight speed of the i -th UAV, and $\theta_i \in [0, 360^\circ)$ represents the horizontal flight direction angle of the i -th UAV. $T_d^{(k)} > 0$ denotes the deployment time of the k -th smoke munition measured from the mission start, and $\Delta d^{(k)} > 0$ denotes the detonation delay time of the k -th smoke munition. The value of the objective function is defined as the integral of the indicator function over the simulation time horizon:

$$f(\vec{X}) = \int_{t_{start}}^{t_{end}} I_{coop}(t, \vec{X}) dt \approx \sum I_{coop}(t_j, \vec{X}) \cdot \Delta t \tag{16}$$

The objective-function value $f(\vec{X})$ must be evaluated numerically by invoking the three-dimensional time-domain simulation model, and no analytical expression with respect to the decision vector $\vec{X}$ can be obtained. Therefore, the objective function $f\left(\vec{X}\right)$ can be regarded as a numerical evaluation of the integral definition of T_e under cooperative conditions.

To verify the reliability of the discretized sampling method, a projection-based obscuration judgment method is further introduced as a reference model. The core idea of this method is to construct a projection plane perpendicular to the missile line of sight, and to project both the cylindrical target and the smoke cloud onto this plane for obscuration evaluation.

Let C_T denote the center of the target and $P_m(t)$ denote the missile position at time t . The direction from the missile to the target can be expressed as

$$\mathbf{d}(t) = \frac{\mathbf{C}_T - \mathbf{P}_m(t)}{\| \mathbf{C}_T - \mathbf{P}_m(t) \|} \tag{17}$$

Accordingly, a projection plane Π perpendicular to $\mathbf{d}(t)$ is constructed as

$$\Pi : \mathbf{d}(t)^\top (\mathbf{x} - \mathbf{P}_0) = 0 \tag{18}$$

where $\mathbf{P}_0$ is a reference point on the plane. For any spatial point $\mathbf{X}$, its perspective projection onto Π can be written as

$$u = \frac{f(\mathbf{X}-\mathbf{P}_m)^\top \mathbf{e}_1}{(\mathbf{X}-\mathbf{P}_m)^\top \mathbf{d}}, v = \frac{f(\mathbf{X}-\mathbf{P}_m)^\top \mathbf{e}_2}{(\mathbf{X}-\mathbf{P}_m)^\top \mathbf{d}} \tag{19}$$

where $\mathbf{e}_1$ and $\mathbf{e}_2$ are two orthogonal basis vectors on Π , and f is a scaling factor.

Using this transformation, the cylindrical target is mapped into a projected region $\mathcal{S}_T$ on the plane, while the smoke cloud is projected as a circular region $\mathcal{S}_S$. The obscuration condition is then defined as

$$\mathcal{S}_T \subseteq \mathcal{S}_S \tag{20}$$

The effectiveness of this reference method is further validated through comparative analysis in Case I, where the results obtained by the two methods are shown to be highly consistent. To address the failure of conventional gradient-based methods in solving this high-dimensional nonlinear optimization problem, as well as the tendency of standard heuristic algorithms to become trapped in local optima, this paper introduces a cooperative-guidance mechanism and a basin-hopping strategy into the standard particle swarm optimization framework, thereby enhancing the algorithm's ability to escape local optima and to explore effective cooperative strategies.

The core idea is that each particle updates its solution by adjusting its position and velocity, and each particle is influenced by both the best solution found by itself and the best solution found by the entire swarm. The velocity update equation is given by:

$$v_i^{(k+1)} = w \cdot v_i^{(k)} + c_1 \cdot r_1 \cdot (p_i^{(k)} - x_i^{(k)}) + c_2 \cdot r_2 \cdot (g^{(k)} - x_i^{(k)}) \tag{21}$$

The position update equation is given by:

$$x_i^{(k+1)} = x_i^{(k)} + v_i^{(k+1)} \tag{22}$$

Here, $v_i^{(k)}$ denotes the velocity of the i -th particle, and $x_i^{(k)}$ denotes the position of the i -th particle. $p_i^{(k)}$ represents the historical best solution of the i -th particle, while $g^{(k)}$ denotes the best global solution. The

parameter w is the inertia weight, which controls the retention of particle velocity. The parameters c_1 and c_2 are the learning coefficients that determine the influence of the individual and the swarm, respectively, and r_1 and r_2 are random variables introduced to enhance search stochasticity. To guide the algorithm toward exploring truly cooperative solutions, the original objective function is modified by introducing a cooperative reward term. The modified fitness function $f_{\text{shaped}}(\vec{X})$ is defined as:

$$f_{shaped}(\vec{X}) = f(\vec{X}) + \beta \cdot N_{contrib}(\vec{X}) \tag{23}$$

Here, $f(\vec{X})$ denotes the true joint effective obscuration duration. $N_{\text{contrib}}(\vec{X})$ is the cooperation factor, representing the number of smoke munitions whose individual effective obscuration duration exceeds a predefined threshold under the given strategy. The parameter β is the cooperative reward coefficient, which is used to regulate the strength of the reward assigned to cooperative behavior.

To avoid repeatedly falling into local optima, a dynamic particle swarm is embedded into a global search framework, namely the basin-hopping algorithm. The core of this algorithm consists of the following three steps:

Step A) Taking the currently obtained best solution $\vec{X}^*_{\text{current}}$ as the starting point, a complete run of the particle swarm optimization algorithm is performed to conduct local intensive exploitation, yielding a local optimal solution $\vec{X}^*_{\text{local}}$.

Step B) The Metropolis criterion is applied to determine whether the current best solution should be updated by $\vec{X}^*_{\text{local}}$. The acceptance probability P_{accept} is defined as:

$$P_{accept} = \begin{cases} 1, & \text{if } F_{shaped}(\vec{X}^*_{local}) \geq F_{shaped}(\vec{X}^*_{current}) \\ \exp\left(\frac{F_{shaped}(\vec{X}^*_{local}) - F_{shaped}(\vec{X}^*_{current})}{T}\right), & \text{otherwise} \end{cases} \tag{24}$$

Step C) A random perturbation is applied to the current solution x_i to generate a new candidate solution x_{local} . The objective function value $f(x_{local})$ is then evaluated, and a decision is made on whether to accept this solution. The algorithm terminates when either the maximum number of iterations is reached or the change in the objective-function value falls below a predefined threshold.

Even when equipped with the proposed improvements, directly applying the particle swarm optimization algorithm to global search over the full decision space still suffers from severe dimensional expansion, which

leads to a rapid growth of the search space and a noticeable degradation in computational efficiency. To achieve a more rational and effective allocation of limited smoke-munition resources, this study introduces an evaluation–allocation–optimization framework that emulates the practical decision-making process in three successive stages. Specifically, the overall operational situation is first assessed to characterize the relative importance of decision targets. Based on the assessment results, available resources are then allocated in a prioritized manner. Finally, the original large-scale optimization problem with multiple objectives and constraints is decomposed into several smaller, logically structured subproblems with reduced computational complexity, from which high-quality optimization solutions can be efficiently obtained.

To support a more rational resource-allocation process, a threat assessment model is constructed to quantify and compare the relative threat levels posed by the three incoming missiles.

$$T_{a,j} = \frac{|\overrightarrow{P_{M_j,0}}| - R_{th}}{v_M} \tag{25}$$

Here, $\vec{P}_{M_j,0}$ denotes the initial position vector of missile M_j , and v_M represents its flight speed. A smaller value of $T_{a,j}$ indicates that missile M_j reaches the threat region at an earlier time, leaving a shorter reaction window for the defense system and thereby implying a higher threat level. Consequently, missiles with smaller $T_{a,j}$ should be assigned higher priority during the resource-allocation process.

During the resource-allocation process, it is also necessary to account for the effectiveness generated by assigning a specific resource to a given target, that is, how much operational benefit can be obtained by allocating resource A to target B . To explicitly incorporate allocation effectiveness into the decision process, a utility function is introduced, and an effectiveness matrix $U_{i,j,k}$ is precomputed to evaluate the interference potential of each smoke munition against each missile. Specifically, the element $U_{i,j,k}$ represents the maximum achievable effective obscuration duration when all k smoke munitions carried by UAV FY_i are allocated to interfere with missile M_j . Its mathematical formulation is given as follows:

$$U_{i,j,k} = \max_{\overrightarrow{X_{i,k}}} f(\overrightarrow{X_{i,k}} \mid FY_i, M_j, k), \forall i \in \{1..5\}, j \in \{1,2,3\}, k \in \{1,2,3\} \tag{26}$$

Here, $f(\cdot)$ denotes the same internal evaluation function as that used in Problem III for computing the joint effective obscuration duration, and $\vec{X}_{i,k}$ represents the deployment strategy vector of UAV FY_i when k smoke munitions are employed.

Finally, a greedy resource-allocation procedure is performed based on the previously obtained evaluation results to generate high-quality smoke-munition deployment decisions. Specifically, a threat-driven greedy strategy guided by the maximum utility value is adopted. Although this approach does not guarantee convergence to the theoretical global optimum and may introduce a certain approximation error, it features a clear decision logic and high computational efficiency, enabling the rapid identification of near-optimal solutions within limited decision time. In this strategy, smoke munitions are allocated sequentially according to the descending order of missile threat levels, and the corresponding decision process is summarized as follows:

Step 1） Initialize the resource pool $\mathcal{F}_a$ by populating it with the five available UAVs and all corresponding smoke munitions.

Step 2）Iterate over all UAVs in the resource pool and their feasible smoke-munition allocation schemes, and evaluate the corresponding predicted utility values.

Step 3） Select the UAV–munition combination that yields the maximum utility value for the current missile:

$$(FY_i^*, k^*) = \arg \max_{FY_i \in \mathcal{F}_a, 1 \le k \le N_{a,i}} U_{i,j,k} \tag{27}$$

Here, $N_{a,i}$ denotes the number of smoke munitions currently available on UAV FY_i .

Step 4）If a positive maximum utility value is identified, execute the corresponding allocation by assigning UAV FY_i^* and its k^* selected smoke munitions, and remove them from the resource pool. Once a UAV is assigned to a specific missile, it is dedicated to that task. This design enables a decomposition of the allocation and continuous optimization processes, reducing problem complexity and improving solution tractability. Once UAV FY_i^* is assigned to missile M_j , its optimal set of k^* smoke munitions is bound to that task. The algorithm may subsequently search for the next best UAV–munition combination among the remaining resources for missile M_j , and this process continues until no UAV in the resource pool can provide a positive utility value for that missile.

Step 5） Proceed to allocate resources to the next target missile according to the predefined threat-ranking order.

In summary, this study addresses the problem of UAV-deployed smoke munitions for missile guidance interference by establishing a unified three-dimensional time-domain modeling and simulation-based optimization framework. For small- to medium-scale operational scenarios, the solution efficiency of particle swarm optimization is enhanced through the introduction of a cooperative reward term and a global perturbation mechanism. For large-scale and highly complex scenarios, a hierarchical evaluation–allocation–optimization strategy is further adopted to decompose the original problem into a set of dimensionally manageable subproblems, thereby significantly improving computational efficiency while preserving the consistency of the underlying model.

SIMULATION EXPERIMENTS

To validate the effectiveness of the proposed model and algorithms, a series of numerical simulations are conducted within a three-dimensional time-domain simulation environment. The main simulation parameters are specified as follows. The speed of the incoming missiles is set to $v_m = 300 \quad m/s$. Each UAV is allowed to deploy two smoke munitions, with a minimum time interval of 1 s between consecutive releases. The minimum time interval of 1 s between consecutive smoke releases is adopted as a simplified operational constraint for modeling purposes and can be adjusted in practical applications according to UAV platform capabilities. The effective radius of the smoke cloud is $R_s = 10 \quad m$, and its effective duration is $T_s = 20 \quad s$. After detonation, the smoke cloud descends vertically at a constant speed of $v_s = 3 \quad m/s$.

A Cartesian coordinate system is established with the decoy target located at the origin, while the real target is modeled as a cylindrical object centered at $(0, 200, 0)$ with a radius of 7 m and a height of 10 m. Three incoming missiles, denoted as M_1 , M_2 , and M_3 , are initially positioned at $(20000, 0, 2000)$, $(19000, 600, 2100)$, and $(18000, -600, 1900)$, respectively. The initial positions of the five UAVs are given by $FY_1(17800, 0, 1800)$, $FY_2(12000, 1400, 1400)$, $FY_3(6000, -3000, 700)$, $FY_4(11000, 2000, 1800)$, and $FY_5(13000, -2000, 1300)$. After receiving mission commands, each UAV determines its flight direction as required and performs straight-line flight at a constant altitude with a speed ranging from 70 to 140 m/s.

Under this unified parameter configuration, five simulation scenarios of increasing complexity are designed to systematically evaluate the proposed methods:

Case I (Fixed-strategy scenario): A single UAV FY_1 is assigned to interfere with a single incoming missile M_1 . The UAV flies toward the decoy target at a fixed speed of 120 m/s. After 1.5 s from mission initiation, one smoke munition is released, with a detonation delay of 3.6 s.

Case II (Single-UAV single-munition optimization): A single UAV FY_1 is assigned to interfere with missile M_1, where the optimization variables include the flight direction and speed of FY_1, as well as the release time and detonation delay of the smoke munition.

Case III (Single-UAV multi-munition cooperation): A single UAV FY_1 is assigned to interfere with missile M_1. The UAV deploys three smoke munitions, and the optimization focuses on the flight parameters of FY_1 as well as the coordinated release and detonation timing of the three munitions.

Case IV (Multi-UAV single-munition cooperation): Three UAVs, $FY_1 - FY_3$, cooperatively interfere with a single missile M_1. Each UAV deploys one smoke munition, and the optimization jointly considers the flight heading and speed of each UAV together with the corresponding munition release and detonation parameters.

Case V (Multi-UAV multi-munition multi-missile scenario): Five UAVs, $FY_1 - FY_5$, are tasked with interfering with three incoming missiles, $M_1 - M_3$. Each UAV is allowed to deploy up to three smoke munitions, and the deployment strategies of all UAVs are jointly optimized.

In Case I, the UAV flies with a prescribed speed and heading and releases a single smoke munition at a predefined time. After a delayed detonation, the smoke cloud is formed and descends vertically at a constant rate.

Figure 1 presents a three-dimensional visualization of the trajectories of the UAV, the missile, and the smoke cloud in this scenario, which clearly illustrates their spatial relationships during the interference process.

Specifically, UAV FY1 departs from the initial position (17800,0,1800) and flies toward the decoy target at a constant speed of 120 m/s. At 1.5 s after mission initiation, the UAV reaches the location (17620,0,1800) and releases the smoke munition. The munition subsequently detonates at 5.1 s from mission start at the position (17188,0,1736.496), generating the smoke cloud that participates in the interference process.

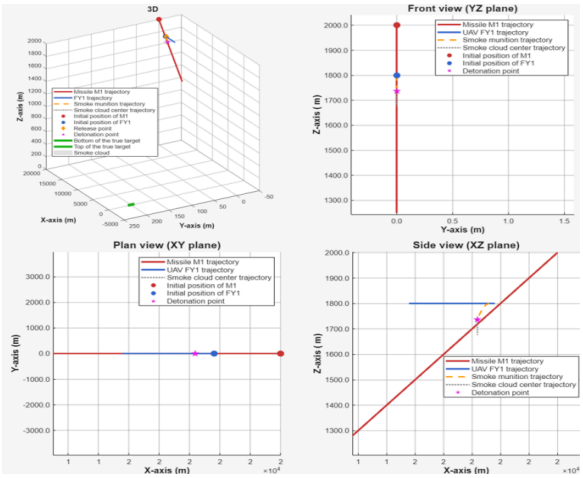

Figure 1. case I UAV–Missile–Smoke trajectories

Building on the trajectory analysis, Figure 2 illustrates the effective shielding time produced by the smoke cloud after detonation during the missile guidance process. It can be observed that, within the 20 s effective lifetime of the smoke cloud, only 1.39 s contributes to effective interference with missile guidance.

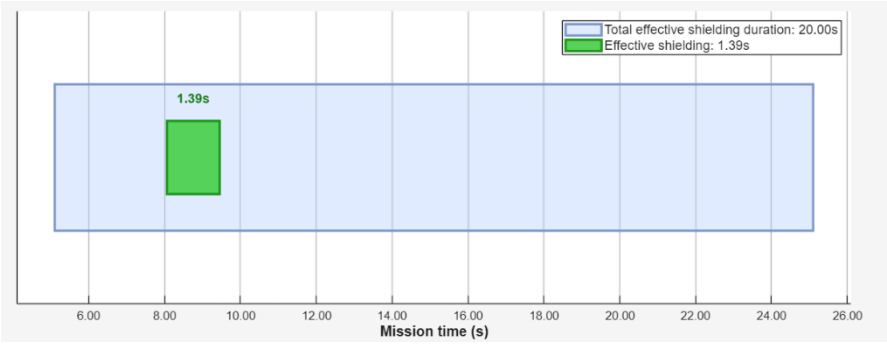

Figure 2. case I Shielding time window

To further validate the accuracy of the discretized sampling method, a comparison with the projection-based obscuration judgment method is conducted for Case I, as illustrated in Figure 3.

As shown in Figure 3, the effective obscuration time intervals obtained by the two methods are highly consistent, with nearly overlapping results in both the onset and duration of the obscuration period. The discretized sampling method yields an effective obscuration duration of 1.39 s, while the projection-based method produces a duration of 1.42 s, resulting in a negligible difference of only 0.03 s.

This comparison demonstrates that the discretized sampling method can provide sufficiently accurate obscuration evaluation, while significantly reducing computational complexity. Therefore, it is adopted in the subsequent optimization scenarios.

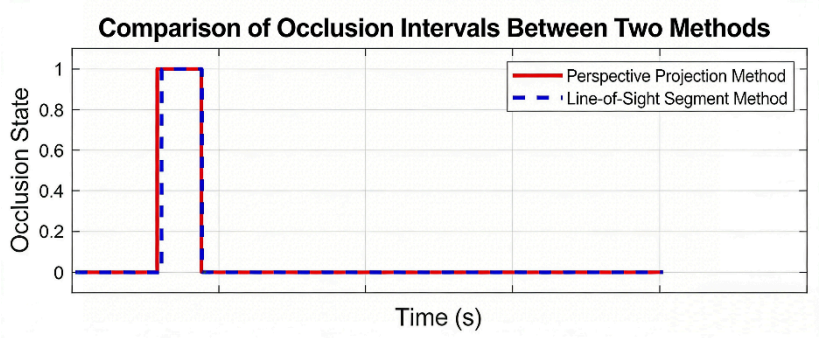

Figure 3. Obscuration interval comparison between two methods in Case I

In Case II, the UAV flight speed and heading, together with the smoke-munition release time and detonation delay, are treated as optimization variables. After 50 iterations of the particle swarm optimization algorithm, the resulting optimal strategy combination is summarized in Table 1:

Table 1. case Ⅱ Optimized UAV and Smoke Munition Parameters

UAV parameter	Smoke munition parameters
UAV speed: $123.65m/s$	Release time: 0.92s
UAV flight direction: $5.07°$	Detonation delay: 0.10s
Smoke munition release coordinates: $(17911.88, 9.92, 1800)$	Detonation coordinates: $(17924.20, 11.01, 1799.95)$

Under the optimized strategy, UAV FY_1 departs from its initial position and performs straight-line flight at a constant speed of 123.65 m/s along the determined heading, with a deflection angle of 5.07° relative to the reference direction. At 0.92 s after mission initiation, the UAV reaches the location $(17911.88, 9.92, 1800)$ and releases the smoke munition. The munition subsequently detonates after a delay of 0.10s at the position $(17924.20, 11.01, 1799.95)$, forming the smoke cloud used for interference. The smoke-deployment trajectories are shown in Figure 4.

With this deployment strategy, an effective interference duration of 4.59 s is achieved. As shown in Figure 5, the interference effect begins at approximately 3 s after mission initiation and provides a continuous and stable shielding window over an extended period. Compared with intermittent obscuration, such sustained shielding is considerably more disruptive to missile guidance systems that rely on continuous target tracking. The corresponding smoke-deployment trajectories further illustrate the effectiveness of the interference process.

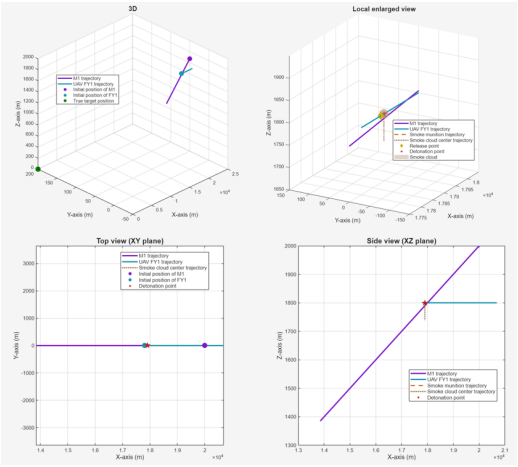

Figure 4. case Ⅱ UAV–Missile–Smoke trajectories

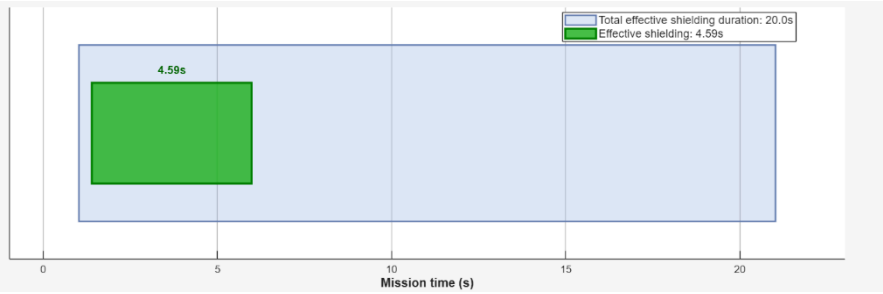

Figure 5. case Ⅱ Shielding time window

For Case III, after ten basin-hopping iterations, the solution converges with an efficient cooperative strategy, as summarized in Table 2. Under this strategy, the UAV flies along the determined heading at a constant speed of 137.1 m/s, with a heading angle of 3.54°. In this flight condition, three smoke munitions are deployed, exhibiting noticeable differences in their spatial positions and resulting shielding effects. Specifically, the three munitions are released at $(17814, 0.85, 1800)$, $(17951, 9.31, 1800)$, and $(19451, 102.4, 1800)$, respectively, and detonate at the corresponding locations $(17828, 1.74, 1800)$, $(17964, 10.15, 1800)$, and $(19465, 102.98, 1800)$. As a result, the first munition provides an effective shielding duration of 3.2 s, the second achieves 4.0 s, while the third does not produce effective obscuration.

Table 2. case Ⅲ Optimized UAV and Smoke Munition Parameters

UAV flight direction	UAV speed	Smoke munition ID	Smoke munition release coordinates	Smoke munition detonation coordinates	Effective shielding duration
3.5395	137.1	1	$(17814, 0.85, 1800)$	$(17828,1,74,1800)$	3.2
3.5395	137.1	2	$(17951, 9.31, 1800)$	$(17964,10.15,1800)$	4
3.5395	137.1	3	$(19451,102.4,1800)$	$(19465,102.98,1800)$	0

From the perspective of individual contributions, the first and second smoke munitions provide shielding durations of 3.2 s and 4.0 s, respectively. However, as indicated by the shielding time-window illustration in Figure 6, a 1.0 s interval is jointly produced by the overlapping effects of the first two munitions. Consequently, the total effective obscuration duration amounts to 6.2 s. The corresponding trajectory visualization shown in

Figure 7 further depicts this interaction process and indicates that the detonation point of the third munition lies outside the effective altitude range required for missile guidance interference.

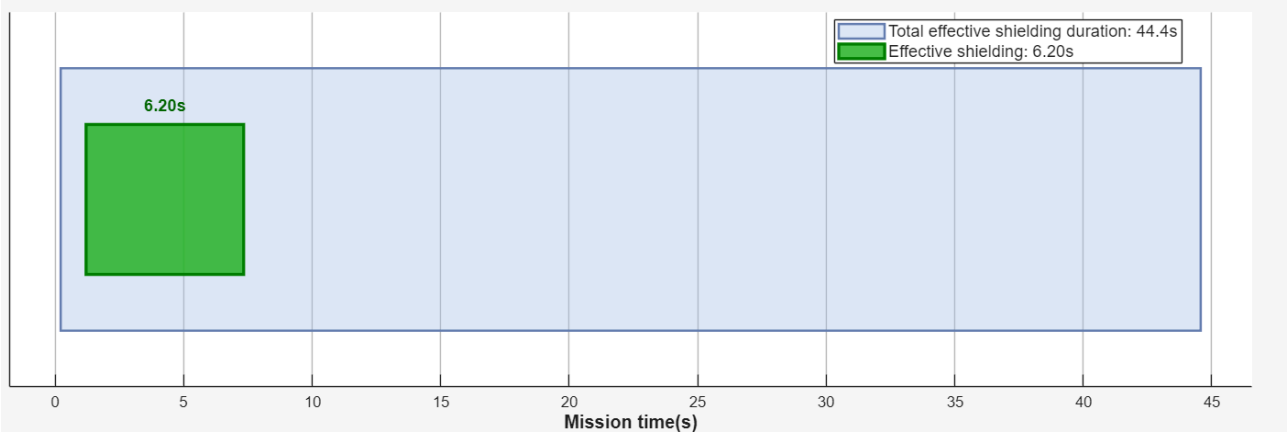

Figure 6. case Ⅲ Shielding time window

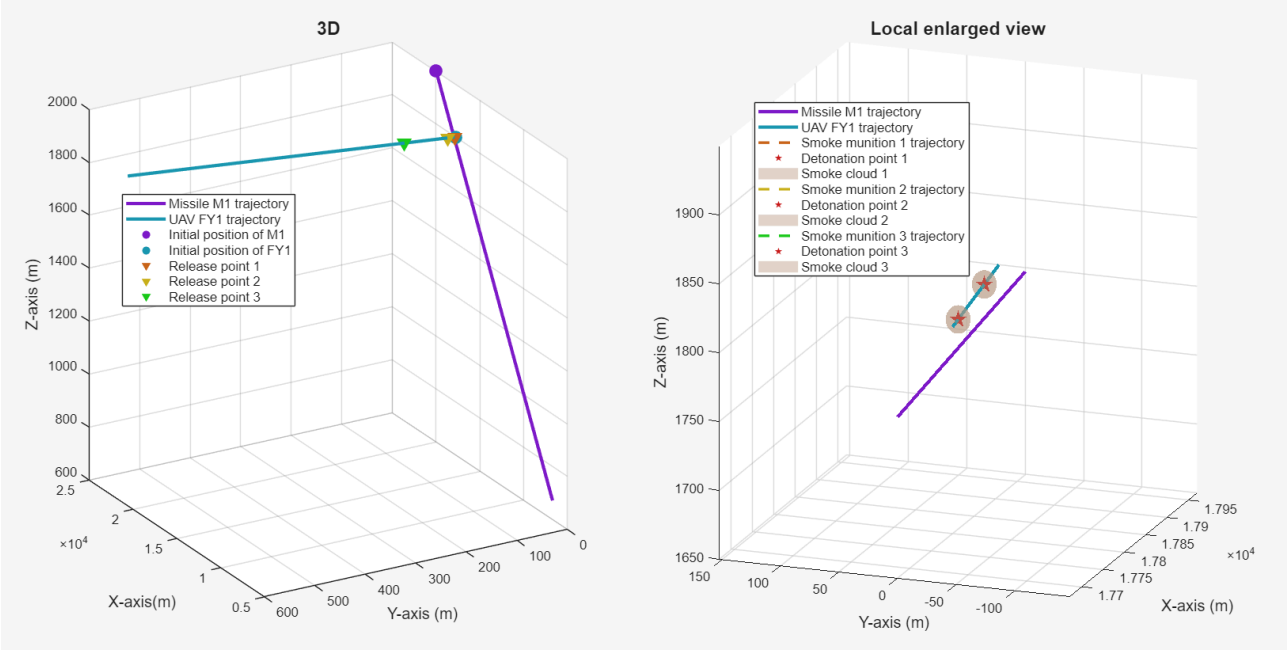

Figure 7. case Ⅲ UAV–Missile–Smoke trajectories

For Case IV, the complex multi-UAV cooperative optimization model converges to an effective coordination strategy after ten basin-hopping iterations guided by the cooperative factor, using the PSO-based metaheuristic framework. The resulting strategy is summarized in Table 3.

In this solution, UAV FY_1 flies at a speed of 114.01 m/s along a heading angle of 6.08°, releases a smoke munition at $(17814, 6.73, 1800)$, and the munition detonates at $(17875, 7.94, 1800)$, yielding an effective

shielding duration of 4.56 s. UAV FY_2 travels at 84.35 m/s with a heading of 271.07°, deploys its munition at $(12016, 541.16, 1400)$, which subsequently detonates at $(12026, 27.28, 1214.5)$, producing a shielding duration of 3.76 s. Similarly, UAV FY_3 flies at 137.09 m/s along a heading of 129.03°, releases its munition at $(4174, -748.25, 700)$, and detonation occurs at $(3466, 125.25, 370.28)$, resulting in an effective shielding duration of 4.56 s.

Table 3. case Ⅳ Optimized UAV and Smoke Munition Parameters

UAV flight direction	UAV speed	Smoke munition ID	Smoke munition release coordinates	Smoke munition detonation coordinates	Effective shielding duration
6.08	114.01	1	$(17814, 6.73, 1800)$	$(17875, 7.94, 1800)$	4.56
271.07	84.35	2	$(12016, 541.16, 1400)$	$(12026, 27.28, 1214.5)$	3.76
129.03	137.09	3	$(4174, -748.25, 700)$	$(3466, 125.25, 370.28)$	2.48

From the effective shielding time axis shown in Figure 8, the relay-like interference process produced by the three smoke munitions can be clearly observed. Under this cooperative strategy, the munitions intermittently interrupt the missile's visual guidance, resulting in a cumulative interference duration of 10.7 s. The corresponding three-dimensional trajectory visualization in Figure 9 further illustrates the coordinated motion and interaction among the three UAVs and their deployed smoke munitions throughout the interference process.

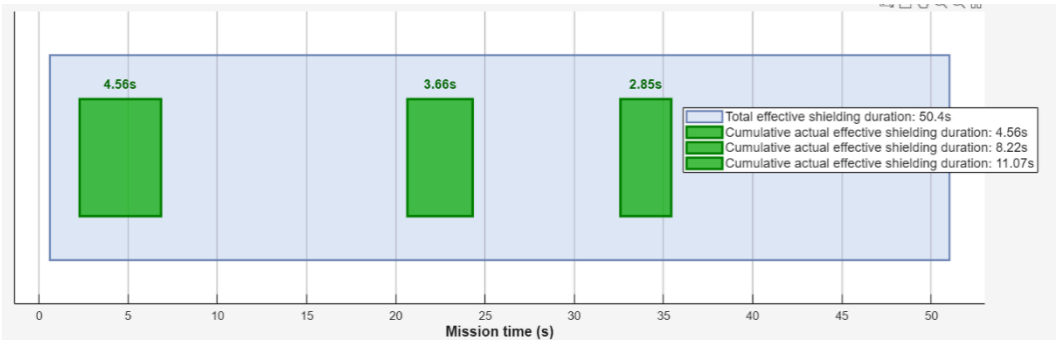

Figure 8. case Ⅳ Shielding time window

It should be noted that the intermittent obscuration observed in this scenario is primarily caused by the non-continuous temporal overlap of multiple smoke clouds. Due to differences in deployment timing, detonation positions, and effective durations, individual smoke munitions generate separate or partially overlapping obscuration intervals, resulting in intermittent blocking of the line of sight. Although such obscuration is not continuous, repeated short-term interruptions can disrupt the missile's target tracking process. In particular, frequent loss and reacquisition of the target may introduce instability in the guidance loop and increase tracking error, thereby reducing the effectiveness of stable target locking.

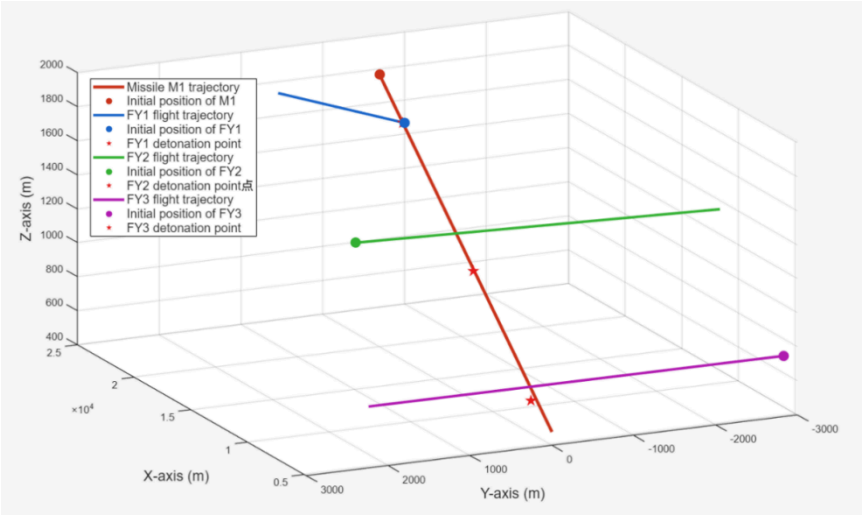

Figure 9. case Ⅳ UAV–Missile–Smoke trajectories

In Case V, the interference of three incoming missiles by five UAVs is considered. The threat levels of the three missiles are first evaluated using the proposed threat assessment model, and the corresponding results are summarized in Table 4. According to the assessment, the threat ranking of the missiles is $M_3 > M_2 > M_1$.

Table 4. Threat Assessment Results

Threat level ranking	M_j	(40)	Time to reach the target area
1	M3		43.70
2	M2		47.08
3	M1		50.33

Based on the threat assessment results, the interference potential of each smoke munition against each missile is further evaluated using the effectiveness assessment model, yielding the corresponding effectiveness

matrix. It is observed that many utility values in the matrix are equal to zero. This outcome arises from the fixed initial positions of the UAVs and missiles, under which certain UAV–missile pairs do not possess feasible spatial configurations for line-of-sight blocking, and thus no effective obscuration can be achieved.

Subsequently, a threat-driven greedy allocation strategy based on the maximum utility criterion is applied, and the resulting allocation scheme is reported in Table 5. The algorithm strictly follows the threat-ranking order $M_3 > M_2 > M_1$ during decision-making. Specifically, the interference potential of all UAVs against missile M_3 is first evaluated. According to the effectiveness matrix, none of the UAVs yields a positive utility value for M_3 , indicating that allocating resources to this missile would not generate effective interference and would therefore be inefficient. The evaluation is then performed on the remaining resources, leading to a final allocation in which FY_1 primarily targets M_1 , FY_2 primarily targets M_2 , and missile M_3 is strategically excluded from interception. The detailed allocation scheme is provided in Table 5:

Table 5. case Ⅴ Optimized UAV and Smoke Munition Parameters

UAV ID	UAV flight direction	UAV flight speed (m/s)	Smoke munition ID	Smoke munition detonation coordinates	Effective interference duration (s)	Target missile ID
FY1	4.1643	140	1	(17829,2.08,1800)	3.3	M1
FY1	4.1643	140	2	(17968,12.2,1800)	3.7	M1
FY1	null	null	3	null	0	null
FY2	301.73	140	1	(13840, −1575, −192)	0	M2
FY2	301.73	140	2	(12594,440.03,1400)	4	M2
FY2	301.73	140	3	(14427, −2525,1119)	0	M2
FY3	0	140	1	(11607, −3000,699)	0	M1
FY3	0	140	2	(17193, −3000, −1260)	0	M1
FY3	null	null	3	null	0	null
FY4	null	null	1	null	0	null
FY4	null	null	2	null	0	null
FY4	null	null	3	null	0	null
FY5	null	null	1	null	0	null
FY5	null	null	2	null	0	null
FY5	null	null	3	null	0	null

After multiple rounds of local refinement and global random perturbation, the final decision strategy is obtained as follows. UAV FY_1 flies at a speed of 140m/s with a heading angle of 4.16°, and releases two smoke munitions at $(17814, 1.02, 1800)$ and $(17954, 11.18, 1800)$, respectively. Through appropriate detonation delays, the munitions detonate at $(17829, 2.08, 1800)$ and $(17968, 12.2, 1800)$, providing effective shield-

ing durations of 3.3s and 3.7s against missile M_1 . UAV FY_2 flies at 140m/s along a heading of 301.73°, deploys a smoke munition at $(12586, 451.94, 1400)$, and detonation occurs at $(12594, 440.03, 1400)$, resulting in a 4.0s interference duration against missile M_2 . In contrast, missile M_3 is strategically excluded from interception. UAVs FY_3 , FY_4 , and FY_5 are retained as standby assets and do not participate in the interception process. Overall, a cumulative interference duration of 11 s is achieved across the incoming missiles. The corresponding three-dimensional trajectories are illustrated in Figure 10, which visually demonstrate the cooperative interception process involving multiple UAVs.

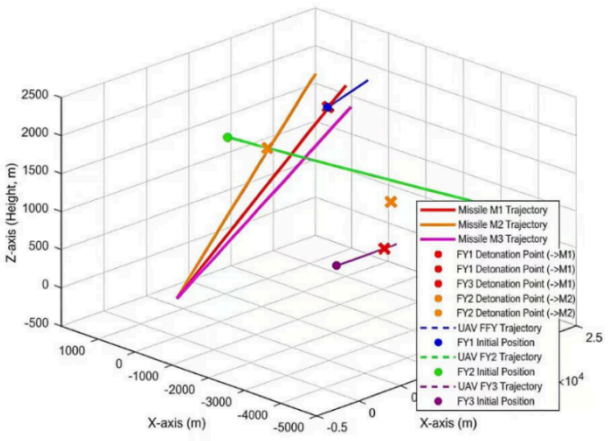

Figure 10. case Ⅴ UAV–Missile–Smoke trajectories

In addition, to evaluate the robustness of the proposed model under perturbations of key parameters, a sensitivity analysis is conducted to examine the influence of several critical factors on the effective shielding duration during the interference process. As illustrated in Figure 11, parameters including the smoke-cloud radius, the descent velocity of the smoke cloud, missile speed, UAV flight speed, smoke release delay, and detonation delay are perturbed in the vicinity of their baseline values. The results indicate that, within reasonable parameter ranges, variations in these key parameters do not alter the fundamental decision outcomes of the model. This demonstrates that the proposed method maintains stable performance under parameter perturbations.

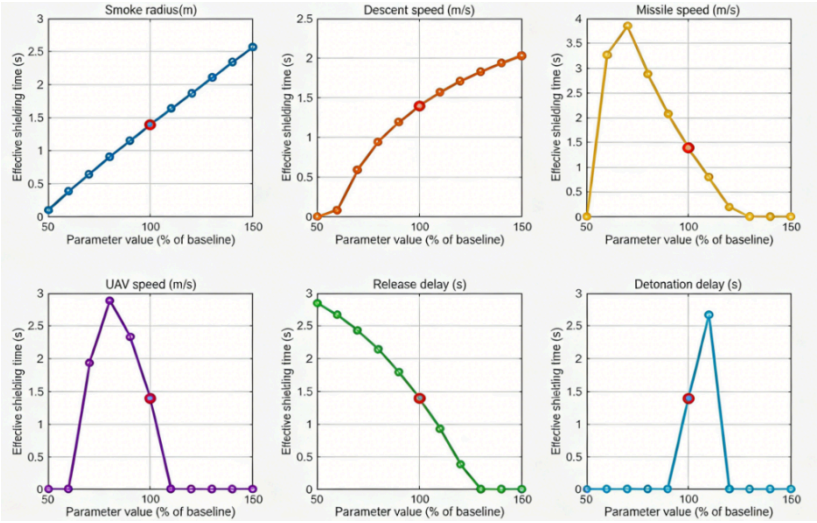

Figure 11. Sensitivity of the model to key parameters

CONCLUSIONS AND FUTURE WORK

From a spatiotemporal coordination perspective, this study systematically investigates the core problem of UAV-deployed smoke munitions for interfering with the guidance processes of incoming missiles, and successfully transforms complex real-world operational scenarios into a three-dimensional time-domain mathematical optimization model. To address highly complex situations involving multi-UAV cooperation and multiple incoming missiles, a hierarchical optimization strategy consisting of threat assessment–resource allocation–local optimization is proposed, enabling the efficient decomposition and solution of decision-making problems under complex constraints. At the algorithmic level, considering the absence of an explicit analytical expression for the objective function and the strong nonlinearity induced by time-domain simulations, a particle-swarm-based solution framework is developed. By incorporating cooperative guidance and global perturbation mechanisms, the proposed approach significantly enhances global search capability and convergence performance in high-dimensional and complex decision spaces, thereby providing effective technical support for the optimization of cooperative UAV interference strategies.

Building upon the findings of this study, several directions merit further investigation. First, the proposed model adopts simplified assumptions with respect to environmental conditions and physical characteristics. Future work may incorporate more realistic factors, such as wind-field distributions and the dynamic diffusion behavior of smoke clouds, to enhance the model's adaptability to real operational environments and improve the accuracy of performance evaluation. Second, the present study focuses on visual obscuration as the primary interference mechanism. The proposed optimization framework can be extended to multimodal

interference scenarios, including radar and infrared domains, thereby broadening the application scope of cooperative interference strategies. Third, the hierarchical optimization strategy developed in this work exhibits strong generality and can be further applied to other cooperative task-planning problems, such as emergency supply delivery, coordinated logistics routing, and collaborative agricultural spraying. By leveraging the modeling principles and optimization approaches presented herein, more effective resource allocation and operational efficiency can be achieved across these application scenarios, which represents an important avenue for future research.

Author Contributions

Conceptualization, Ma M S and Tian H J; methodology, Ma M S; software, Ma M S; validation, Ma M S; formal analysis, Ma M S; investigation, Ma M S; writing—original draft preparation, Ma M S, Zhu T; writing—review and editing, Ma M S and Tian H J; supervision, Tian H J and Liu G J. All authors have read and agreed to the published version of the manuscript.

Conflicts of Interest

The authors declare no conflict of interest.

Funding

This work is supported by the National Natural Science Foundation of China with the Grant No. 62303108 and the Supporting Project number (D-8006-23-0223).

Acknowledgements

This work was supported by the National Natural Science Foundation of China (Grant No. 62303108) and the Supporting Project (No. D-8006-23-0223). The authors would also like to thank the editor and the anonymous reviewers for their valuable comments and suggestions, which have helped improve the quality of this manuscript.

Data Sharing Agreement

The datasets used and/or analyzed during the current study are available from the corresponding author on reasonable request.

REFERENCES

[1] Quang S D, Nguyen Van T, Nguyen Trung T. Obscurant and radiation characteristics of infra-red-screening smoke composition based on red phosphorus. Defence Science Journal. 2022; 72(3):353-358. doi: 10.14429/dsj.72.17676

[2] WANG G, LV X, CUI L Z, YAN X H. The methods of task pre-allocation and reallocation for multi-UAV cooperative reconnaissance mission. IET Collaborative Intelligent Manufacturing. 2023; e12090. doi: 10.1049/cim2.12090

[3] MENG Q C, CHEN K, QU Q J. PPSwarm: Multi-UAV path planning based on hybrid PSO in complex scenarios. Drones. 2024; 8: 192. doi: 10.3390/drones8050192

[4] CHEN X, LIU Y T, YIN L Y, QI L J. Cooperative task assignment and track planning for multi-UAV attack mobile targets. Journal of Intelligent & Robotic Systems. 2020; 100(1): 45-63. doi: 10.1007/s10846-020-01241-w

[5] CAO M L, PENG J Y, LIU Y, YIN Y. Multi-UAV task allocation and path planning in emergency rescue scenarios with uncertain requirements. Journal of Industrial and Management Optimization. 2025; 21(10): 6107-6133. doi: 10.3934/jimo.2023102

[6] GUO C, HUANG L, TIAN K. Combinatorial optimization for UAV swarm path planning and task assign-ment in multi-obstacle battlefield environment. Applied Soft Computing. 2025; 171: 112773. doi: 10.1016/j.asoc.2024.112773

[7] XU L, CAO X B, DU W B, LI Y M. Cooperative path planning optimization for multiple UAVs with com-munication constraints. Knowledge-Based Systems. 2023; 260: 110164. doi: 10.1016/j.knosys.2022.110164

[8] CRUZ J B, CHEN G, LI D X, WANG X. Particle swarm optimization for resource allocation in UAV coop-erative control. In AIAA Guidance, Navigation, and Control Conference and Exhibit; 16-19 Aug 2004; Providence, RI, USA. Reston, VA: American Institute of Aeronautics and Astronautics; 2004. p. AIAA 2004-5250. doi: 10.2514/6.2004-5250

[9] GUO J, GAN M G, HU K. Cooperative path planning for multi-UAVs with time-varying communication and energy consumption constraints. Drones. 2024; 8: 654. doi: 10.3390/drones8110654

[10] Oh G T, Kim Y D, Ahn J M, CHOI H L.PSO-based optimal task allocation for cooperative timing missions. In: IFAC Symposium on Automatic Control in Aerospace; 30 Aug-2 Sep 2016; Sherbrooke, QC, Canada. Laxenburg, Austria: IFAC; 2016. p. 314-319. doi: 10.1016/j.ifacol.2016.09.054

[11] YAN F, CHU J, HU J W, ZHU X P. Cooperative task allocation with simultaneous arrival and resource constraint for multi-UAV using a genetic algorithm. Expert Systems With Applications. 2024; 245: 123023. doi: 10.1016/j.eswa.2023.123023

[12] HE W J, QI X G, LIU L F. A novel hybrid particle swarm optimization for multi-UAV cooperate path planning. Applied Intelligence. 2021; 51(6): 4028-4051. doi: 10.1007/s10489-020-02089-7

[13] ZHANG B R, HUANG K, CHEN Y J, YANG D C. Task allocation and trajectory optimization for multi-UAV cargo systems with cellular-connected constraints. IET Communications. 2025; 19: e70106. doi: 10.1049/cmu2.70106

[14] LEE D H, ZAHEER S A, KIM J H. A resource-oriented, decentralized auction algorithm for multirobot task allocation. IEEE Transactions on Automation Science and Engineering. 2014; 12(1): 1-13. doi: 10.1109/TASE.2014.2361334

[15] JEON H M, LIM J W, RYOO C. Task assignment for multiple multi-purpose unmanned aerial vehicles using greedy algorithm. International Journal of Aeronautical and Space Sciences. 2024; 25: 1380-1394. doi: 10.1007/s42405-023-00645-8

[16] TAN Y F, ZHOU C, QIAN F. Cooperative task allocation method for multi-unmanned aerial vehicles based on the modified genetic algorithm. IET Intelligent Transport Systems. 2024; 18: 1164-1173. doi: 10.1049/itr2.12374

[17] XIONG Y T, ZHANG L. Multi-UAV task allocation based on grid-based particle swarm and genetic hy-brid algorithm. Mathematics. 2025; 13: 3591. doi: 10.3390/math13203591

[18] WANG R, SHAN Y Q, SUN L W, SUN H. Multi-UAV cooperative task allocation based on multi-strategy clustering ant colony optimization algorithm. ICCK Transactions on Intelligent Systematics. 2025; 2(3): 149-159. doi: 10.12142/ICCK.2025.020303

[19] ZHANG R, CHEN X, LI M Y. Multi-UAV cooperative task assignment based on multi-strategy improved DBO. Cluster Computing. 2025; 28: 195. doi: 10.1007/s10586-024-04512-3